Transportation Research Part C 68 (2016) 144–159

Contents lists available at ScienceDirect

Transportation Research Part C

journal homepage: www.elsevier.com/locate/trc

Online calibration for microscopic traffic simulation and dynamic multi-step prediction of traffic speed ☆

Vasileia Papathanasopoulou, Ioulia Markou, Constantinos Antoniou *

National Technical University of Athens, Zografou GR-15780, Greece

ARTICLE INFO

Article history:
Received 21 June 2015
Received in revised form 5 April 2016
Accepted 5 April 2016
Available online 11 April 2016

Keywords:
Speed prediction
Traffic simulation
Car-following models
Dynamic calibration

ABSTRACT

Simulating driving behavior in high accuracy allows short-term prediction of traffic parameters, such as speeds and travel times, which are basic components of Advanced Traveler Information Systems (ATIS). Models with static parameters are often unable to respond to varying traffic conditions and simulate effectively the corresponding driving behavior. It has therefore been widely accepted that the model parameters vary in multiple dimensions, including across individual drivers, but also spatially across the network and temporally. While typically on-line, predictive models are macroscopic or mesoscopic, due to computational and data considerations, nowadays microscopic models are becoming increasingly practical for dynamic applications. In this research, we develop a methodology for online calibration of microscopic traffic simulation models for dynamic multi-step prediction of traffic measures, and apply it to car-following models, one of the key models in microscopic traffic simulation models. The methodology is illustrated using real trajectory data available from an experiment conducted in Naples, using a well-established car-following model. The performance of the application with the dynamic model parameters consistently outperforms the corresponding static calibrated model in all cases, and leads to less than 10% error in speed prediction even for ten steps into the future, in all considered data-sets.

1. Introduction

Developments of Advanced Traveler Information Systems (ATIS) rely significantly on the capability to perform accurate estimates of the current traffic state and short-term predictions of driving behavior and traffic characteristics, such as speed (Vlahogianni et al., 2005; van Lint et al., 2005; Vlahogianni et al., 2008). Due to a number of practical, data and computational considerations, during the past two decades, ATIS applications have been mostly supported by mesoscopic or macroscopic traffic simulation models. Data collection and computational advances are making it possible to consider more detailed, microscopic models for this kind of applications. Naturally, such models introduce a number of complications, and therefore their adoption should be clearly motivated and justified.

While such systems have been around for decades, current developments, such as the increasing interest in Active Traffic Management, make them more relevant (Kurzhanskiy and Varaiya, 2010). Indeed, ATIS can be effective in supporting active traffic management policies by Real-Time Decision Support Systems, whose core engine is a real-time traffic simulation model. The real-time requirements bring to the forefront the limitations of static calibration, and accelerate the need for

☆ This article belongs to the Virtual Special Issue on Recent Advances in Transportation Management and Control.

* Corresponding author.
E-mail address: antoniou@central.ntua.gr (C. Antoniou).

http://dx.doi.org/10.1016/j.trc.2016.04.006
0968-090X/© 2016 Elsevier Ltd. All rights reserved.

procedures like the ones discussed in this research. An example of such applications is the Integrated Corridor Management initiative in the US (Miller and Skabardonis, 2010).

Simulation models do not always adequately reflect field conditions outside of the time period for which they have been calibrated (Balakrishna et al., 2007; Daamen et al., 2014; Henclewood et al., 2012). Microscopic models often comprise different detailed models, including car-following, lane-changing and gap-acceptance models. In most cases, the parameters of these models are assumed to be stable, both across space and time, and also across drivers. The online calibration of car-following models is a promising approach to capture the heterogeneity of driver behavior and traffic conditions. By continuously supplying a car-following model with surveillance data, an online calibration process could be applied in order to adapt model parameters to the current traffic state. In this view, the use of richer data, such as real-time Floating Car Data (FCD), based on traces of Global Navigation Satellite Systems (GNSS), could be leveraged as a reliable and cost-effective way to gather accurate traffic data (De Fabritiis et al., 2008; Antoniou et al., 2011).

Calibration of car-following models (Brackstone and McDonald, 1999) has been an issue for a long time (Aycin and Benekohal, 1999), but nowadays it has received a new boost (Hoogendoorn and Hoogendoorn, 2010; Monteil et al., 2014), in light of new data-collection techniques, mostly related to the increasing availability of trajectory data (Kesting and Treiber, 2008; Punzo et al., 2005; Papathanasopoulou and Antoniou, 2015), which of course introduce other challenges (Punzo et al., 2012).

Online calibration has been used in many macroscopic and mesoscopic modeling approaches (Papageorgiou et al., 1989; Kim, 2002; Antoniou et al., 2005; Fei et al., 2011). The use of the Kalman Filter (and its extensions) for online parameter calibration has shown encouraging results (Antoniou et al., 2007). However, in recent years there has been an increasing interest in online applications of microscopic traffic models. Moreover, Henclewood et al. (2012) suggest that a real-time calibration algorithm should be included in online, data-driven microscopic traffic simulation tools.

The objective of this paper is to motivate, develop and demonstrate with real data a practical approach for the online calibration of microscopic traffic simulation models, which considers dynamic parameters for individual drivers, in time and space. At each time instance, the dynamically obtained model parameters are being used for short-term prediction (up to ten steps into the future), and the performance of this prediction is compared with the reference case of static model parameters.

This paper presents an alternative methodology for microscopic online calibration and multiple step prediction and is organized as follows. Firstly, a literature review is presented in the following section. Then, the overall methodological framework is presented. A case study setup to demonstrate the feasibility and superiority of the approach, over previous techniques, is then presented, followed by the presentation of the dynamic calibration procedure and an analysis of the results. A discussion of the results follows in the concluding section, and future prospects are proposed.

2. Literature review

Reliable representation of driving behavior is a crucial issue for traffic simulation. Appropriate simulation models are chosen according to the requirements of each application; when considering the modeling detail, traffic simulation models can be divided into microscopic, mesoscopic and macroscopic. Microscopic models provide the highest level of detail for advanced transport applications (Antoniou and Koutsopoulos, 2006). However, the traditional static calibration approach may not allow the incorporation of driving heterogeneity in the simulation.

In recent years there has been a tendency towards more flexible and dynamic methods than static car-following models. It is widely accepted that driving behavior in general (and therefore car-following parameters) vary in multiple dimensions, i.e. exhibit inter-personal, temporal and spatial heterogeneity. Higgs and Abbas (2014) compare car-following models at different levels of analysis: driver, car-following period and cluster of drivers. For example, Ossen and Hoogendoorn (2005) have identified considerable differences between the car-following behavior of individual drivers. Ma (2006) has developed a neural fuzzy framework for modeling car-following behavior. It illustrates human knowledge of car-following in a more understandable manner and can be rather flexible as the regime parameters and model forms may vary according to the application context. According to Hoogendoorn et al. (2006) and Ellison et al. (2013), real driving behavior is variable in time and space. Some researchers have attempted to capture heterogeneity across drivers spatially (e.g. Papathanasopoulou and Antoniou (2015)) or temporally, which is one of the aspects investigated in this research.

Many car-following models predict a stable car-following behavior with a very small fluctuation around an equilibrium value. However, in reality these fluctuations are much larger than these models predict. Wagner (2012) has attributed them not due to driver heterogeneity, but to an internal stochasticity of the driver itself. Randomness is thus incorporated in traffic flow and model calibration requires the flexibility to adapt to it. On the other hand, several empirical analyses performed by Ossen and Hoogendoorn (2007) showed a high degree of driver heterogeneity in car-following. Inter-driver differences could be described not only by different parameter values, but also different model specifications may be needed. All above researchers conclude that different optimal parameter values, as well as different optimal car-following models, should be applied to overcome this problem.

Static calibration requires a database with historical data. It could feed a simulation model with initial parameter values, which allow a good representation of a general traffic state (Balakrishna, 2006). However, dynamic calibration could take advantage of real-time data and adapt model parameters to the current traffic state. Dynamic estimation of model parameters and especially reaction time have been attempted by e.g. Hoogendoorn et al. (2006) and Ma and Jansson (2007). Hoogendoorn et al. (2006) and Lorkowski and Wagner (2005) use the Unscented Kalman Filter (UKF), while Ma and Jansson (2007) have proposed a dynamic model estimation method based on iterative usage of the Extended Kalman Filter (IEKF) algorithm. Ma and Andréasson (2005) have suggested a dynamic car following data collection and noise cancellation based on the Kalman smoothing. However, according to Treiber and Kesting (2013), smoothing the data had no significant influence on the calibration quality. Naturally, calibration and sampling issues in estimation car-following parameters have been studied extensively in the literature (Monteil et al., 2014; Schultz and Rilett, 2004).

Rahman et al. (2014) develop a calibration approach based on the Markov Chain Monte Carlo (MCMC) simulation that uses the Bayesian estimation theory. The authors use a linear model (Helly) with a different number of vehicle trajectories on a highway network. Ossen and Hoogendoorn (2011) investigate the level of heterogeneity in car-following behavior, using a large number of trajectory observations collected via helicopter. The authors observe different vehicle type interactions and develop eight models with different car-following assumptions.

3. Methodology

In this research, a methodological framework for the dynamic calibration of car-following models using real-time data is proposed. The approach has two main steps, an estimation phase and a prediction phase. The estimation phase relies on a constrained global optimization algorithm. Once an optimal set of parameters is identified for each individual time-instance (and each individual driver), multi-step prediction is performed. In each time step, prediction is achieved using the estimated values from the previous time step, i.e. the best available estimates of the drivers' behavior. The evolving patterns of the driver behavior during the past few intervals is used to forecast the expected behavior during the next few time-steps. Naturally, this logic could be adapted to data-availability or computational concerns, e.g. it could only be invoked when there is an indication that traffic conditions may be changing (e.g. automatically detected anomaly in the data).

The dynamic calibration problem can be mathematically stated as

$$\min f(\mathbf{x_t}), \quad \mathbf{x_t} = (x_{1t}, \dots, x_{nt}) \in \mathcal{R}^n \tag{1}$$

where $f(\mathbf{x_t})$ is the objective function (e.g. error estimating the difference between observed and simulated values of a traffic measure), t is the current time interval, $\mathbf{x_t}$ stands for time dependent parameters, and the feasible region $\mathcal{F}$ is defined by

$$\mathcal{F} = \{\mathbf{x_t} \in \mathcal{R}^n | g_j(\mathbf{x_t}) \leqslant 0 \quad \forall j\} \tag{2}$$

where $g_j(\mathbf{x_t}), \quad j = 1, \dots, m$ are inequality constraints. For instance, these constraints could ensure that a traffic measure, such as space gaps, will not take unacceptable values. The way that the constraints are handled may vary according to the type of optimization algorithm that is adopted, including the penalty function method, special representations and operators, and the co-evolutionary method, the repair method or the multiobjective method (Runarsson and Yao, 2005). The dynamic calibration problem could also be stated as a multiobjective optimization problem including various measures of effectiveness (such as speeds, space gaps, and accelerations) and various measures of goodness-of-fit (such as normalized root mean square error and mean prediction error, as described in Section 4.3).

$$\min(f_1(\mathbf{x_t}), f_2(\mathbf{x_t}), \dots, y_1(\mathbf{x_t}), y_2, (\mathbf{x_t}) \dots z_1(\mathbf{x_t}), z_2, (\mathbf{x_t}), \dots), \quad \mathbf{x_t} = (x_{1t}, \dots, x_{nt}), \in \mathcal{R}^n \tag{3}$$

where $f_1(\mathbf{x_t}), f_2(\mathbf{x_t}), \dots$ correspond to the same measure of effectiveness (e.g. comparison of observed and simulated speeds), but different measures of goodness-of-fit, while $f_i(\mathbf{x_t}), y_i(\mathbf{x_t}), z_i(\mathbf{x_t}) \dots$ correspond to different measures of goodness-of-fit, but for the same measure of effectiveness.

The estimated model parameters can then be easily propagated into the future, thus providing plausible predictions of these values for the next intervals, as shown in Fig. 1 for a hypothetical parameter. A general way to express this evolution could be

$$\hat{\mathbf{x}}_{t+1} = h(\mathbf{x}_t, \mathbf{x}_{t-1}, \mathbf{x}_{t-2}, \dots) \tag{4}$$

where h is a function relating an estimate of the car-following model parameter values in the next time interval to the best available estimates of the same model parameters in previous time steps. However, in this way all observations from time $t = t_0$ up to time t are considered as equally important and included to define the objective function. This approach could lead to errors since drivers may drive in a different way at the current moment in comparison with previous time instants. The apparent solution could be based on weighting the data:

$$\hat{\mathbf{x}}_{t+1} = h(w_0 \cdot \mathbf{x}_t, w_1 \cdot \mathbf{x}_{t-1}, w_2 \cdot \mathbf{x}_{t-2}, \dots) \tag{5}$$

where w_i are the weights of observations. Presumably largest weights would be applied to the most recent data and therefore $w_1 > w_2 > w_3 > \cdots$. The decaying weights thus imply that in practice only a finite number of past observations affects the process. A more explicit example of an operationalization of this process is e.g. an autoregressive process, such as:

$$\hat{\mathbf{x}}_{t+1} = f_0 \cdot \mathbf{x}_t + f_1 \cdot \mathbf{x}_{t-1} + f_2 \cdot \mathbf{x}_{t-2} + \epsilon \tag{6}$$

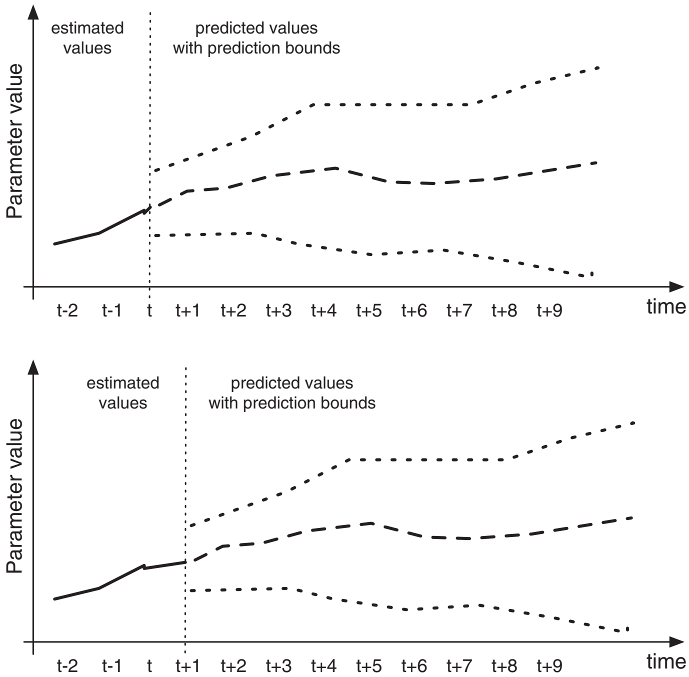

Fig. 1. A rolling horizon for prediction with improving bounds.

where f_i are the autoregressive factors, and ϵ a random error term. A process for determining these factors is presented e.g. in (Antoniou, 2004, p. 79).

Through repeating this process, multi-step predictions can be obtained in the following manner:

$$\hat{\mathbf{x}}_{t+2} = h(w_0 \cdot \hat{\mathbf{x}}_{t+1}, w_1 \cdot \mathbf{x}_t, w_0 \cdot \mathbf{x}_{t-1}, \ldots) \quad (7)$$
$$\hat{\mathbf{x}}_{t+3} = h(w_0 \cdot \hat{\mathbf{x}}_{t+2}, w_1 \cdot \hat{\mathbf{x}}_{t+1}, w_2 \cdot \mathbf{x}_t, \ldots) \quad (8)$$

Naturally, as the number of time-intervals (for which the prediction is performed) increases, the accuracy of these predictions is expected to deteriorate, as evidenced schematically by the widening bounds of the predicted values in Fig. 1. A practical way to determine these bounds is presented in Pereira et al. (2014). As the process is repeated, though, when new data are available, these forecasts can be improved, as shown by the lower subfigure in Fig. 1. This concept of “rolling horizon” is being used in software for real-time traffic predictions (Ben-Akiva et al., 2010). In that case, at time $t + 1$ the previously predicted values of the model parameters for time $t + 1$ can now be estimated using available data. Furthermore, the previous two-step predicted model parameters for time interval $t + 2$ can now be replaced by one-step predicted model parameters, since estimates of the model parameters are available up to time interval $t + 1$. Similarly, e.g. at time $t + 1$ for time interval $t + 7$, the previous seven-step prediction (using estimated values up to time interval t and predicted parameter values for subsequent intervals) can be replaced by an –arguably more accurate– six-step prediction (using estimated values up to time interval $t + 1$ and predicted parameter values for subsequent intervals).

The proposed methodological framework may benefit from a system that allows a fleet of connected vehicles to exchange information, such as (X, Y, Z) coordinates, using a central data system. However, even a single instrumented vehicle, with the ability to geo-locate itself, and obtain (e.g. via suitable instruments and cameras) estimates of the speed and distance of surrounding vehicles, has access to all information required to apply this methodology. Therefore, speeds, accelerations or gaps could be calculated per time instant and used to dynamically calibrate driver-specific, time-varying parameters for the considered model. The overall methodology is illustrated in Fig. 2. A calibration process is demonstrated for each time instant t, using observations available up to that time and applying a suitable optimization algorithm, solving Eqs. (1) or (3). The estimated optimal model parameters for time intervals up to t are being used to predict dynamic parameter values for the subsequent intervals, using Eqs. (4) or (5) and so on. These predicted parameters can then be used as time-dependent inputs into the microscopic traffic models to provide predicted outputs for the horizon from t onwards. In the next time-interval, this process is repeated, but this time using also measured information from time-interval $t + 1$, thus obtaining an estimated set of model parameters for time interval $t + 1$, updated predicted values for the subsequent intervals, plus a new predicted value for a new time-interval (for example, if performing n-step prediction, during time t we obtained predicted parameter values for intervals $t + 1$ through $t + n$, but when we move to time interval $t + 1$ then we obtain predictions for intervals $t + 2$ through $t + n + 1$, thus revising the previous estimates for intervals $t + 2$ through $t + n$ and extending our prediction horizon to $t + n + 1$).

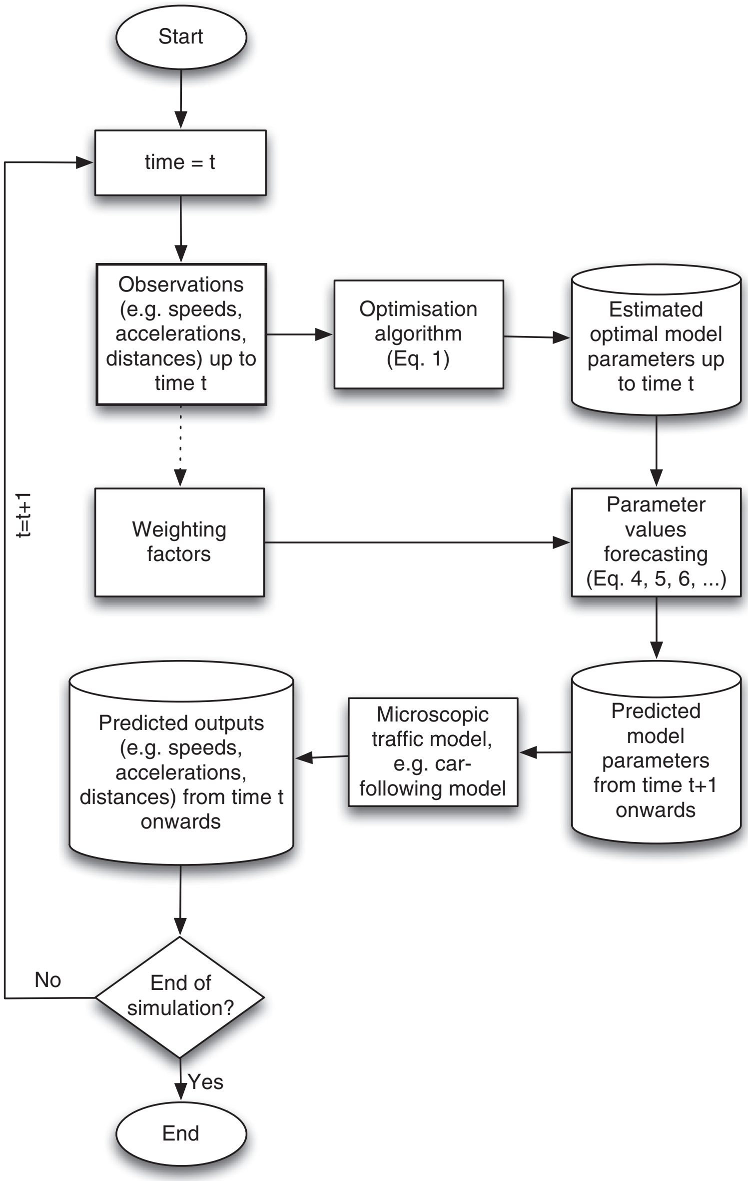

Fig. 2. Methodological overview: dynamic calibration and multiple steps prediction.

4. Case study setup

The methodology is applied to a car-following model, which is arguably the most critical component of microscopic traffic simulation models. In particular, Gipps' model (used e.g. in the widely used Aimsun traffic simulation model) is calibrated using available data from an experiment conducted in Naples (Punzo et al., 2005). A static calibration is also performed in order to be used as a reference benchmark. The main difference from dynamic calibration is that the parameter values are constant for all the time instants and all prediction steps. For both methods, the same optimization algorithm was used. Therefore, for the static calibration Eq. (1) is simplified through the removal of subscript t, while of course the forecasting Eq. (4) and so on are not relevant (since the parameter values are constant).

4.1. Description of Gipps' model

The car-following model, used in Aimsun, is a safety distance model based on the model developed by Gipps (Gipps, 1981; Olstam and Tapani, 2004; Barceló et al., 2005). The model suggests that the speed of a vehicle (n) is subject to three constraints (Eq. (9)). First, the vehicle speed does not exceed the driver's desired speed (V_n). Second, the vehicle accelerates rapidly until it approaches the desired speed and then the acceleration is reduced almost to zero. If two vehicles are far apart, they behave as in the free flow condition. These two conditions are summarized in the first part of Eq. (9). The third condition is taken into account, when the vehicle is constrained by the vehicle in front. It is taken for granted that the following vehicle will adjust its velocity so as to keep a safe distance from the preceding vehicle. This condition is described by the second part of Eq. (9). Overall, according to the above restrictions, the speed of vehicle n at time $(t+\tau)$ could be calculated by the following formula:

$$v_n[t+\tau] = min\begin{cases} v_n[t] + 2.5 \cdot a_n \cdot \tau \cdot \left(1 - \frac{v_n[t]}{V_n} \cdot \sqrt{\left(0.025 + \frac{v_n[t]}{V_n}\right)}\right) \\ b_n \cdot \tau + \sqrt{(b_n \cdot \tau)^2 - b_n \cdot \left[2 \cdot (x_{n-1}[t] - s_{n-1} - x_n[t]) - v_n[t] \cdot \tau - \frac{v_{n-1}^2[t]}{\hat{b}}\right]} \end{cases} \tag{9}$$

where

a_n: the maximum acceleration that the driver of vehicle n wishes to acquire (m/s^2).
b_n: the maximum braking that the driver of vehicle n wishes to apply in order to avoid a crash, $b_n<0$ (m/s^2).
$\hat{b}$: the estimated maximum braking that the driver of the preceding vehicle $(n-1)$ wishes to apply (m/s^2).
$s_{n-1} = L_{n-1}$ + safety, namely the size of the preceding vehicle $(n-1)$ including its length and the safety distance at which vehicle n is unwilling to compromise even when at rest (m).
V_n: the speed at which the driver of vehicle n wishes to travel (m/s).
$x_n[t]$, $x_{n-1}[t]$: the location of the front side of the respective vehicle (n or $n-1$) at time t (m).
$v_{n-1}[t]$: the speed of the preceding vehicle $(n-1)$ at time t (m/s).
$v_n[t]$: the speed of the following vehicle (n) at time t (m/s).
τ: the apparent reaction time (a constant for all vehicles) (s).

4.2. Data

A series of data-collection experiments were carried out on roads surrounding the city of Naples, in Italy (Punzo et al., 2005). All data were collected under real traffic conditions in October 2002. All data were collected from the same platoon, namely the same four drivers by the same vehicles (vehicles 1, 2, 3, 4) moving in the same sequence (first vehicle 1 as the leader, followed by vehicle 2, which was in turn followed by vehicle 3, while the last vehicle was vehicle 4), but from different driving sessions, outlined in Table 1. The driving routes and traffic conditions were differentiated among the datasets. Datasets with index A and C correspond to one-lane urban road, while datasets with index B to a two-lane extraurban highway. However, all selected roads have one lane per direction in order to avoid effects on driving behavior by lane changing. GPS receivers located on the vehicles were recording the coordinates X, Y, Z of each vehicle per 0.1s (i.e. in 10 Hz). Thus, the speed of each vehicle ($v_1(t), v_2(t), v_3(t), v_4(t)$) and the travelled distances for each vehicle could be calculated at each moment ($x_1(t), x_2(t), x_3(t), x_4(t)$). In this research, data used are readily available observations from the field. No corrections and no interpolation have been performed. Therefore, only segments with consecutive measurements have been considered. A detailed description of the data could be found in Punzo et al. (2005), who kindly provided the data for this research.

4.3. Measures of goodness-of-fit

The performance of the models presented in this paper is evaluated using several goodness-of-fit measures: RMSN, RMSPE, MPE and Theils U, U_m and U_s coefficients (for details and a discussion of these metrics, see e.g. Antoniou et al. (2013)). Different measures are used so that the properties of the calibration and validation results could be quantified from different views. For example, the normalized root mean square error (RMSN) assesses the overall error and performance of each method estimating the difference between the observed values Y_n^{obs} and their simulated counterparts Y_n^{sim}. The root mean square percentage error (RMSPE) penalizes large errors more heavily than small errors and the mean prediction error (MPE) indicates the existence of systematic under- or over-estimation in the simulated values. The measure of Theil's

Table 1
Speed profile and experimental data.

Data series	Length (s)	Summary statistics of speed (m/s)			
		min	max	mean	var
B1695	169.5	0.11	19.00	12.18	14.27
A358	35.8	3.35	13.22	9.10	12.16
A172	17.2	6.16	9.10	7.51	0.97
C168	16.8	9.74	12.86	11.18	0.50
C171	17.1	2.94	9.82	6.08	4.16

inequality coefficient U has been applied in transport model validation and includes three error proportions: the bias (U_m), the variance (U_s) and the covariance (U_c), whose sum is one. Values close to zero for U_m and U_s measures indicate an ideal fit, while values close to 1 suggest the worst fit. The goodness-of-fit measures are calculated from the following equations:

$$\mathrm{RMSN} = \frac{\sqrt{N \cdot \sum_{n=1}^{N} \left(Y_n^{sim} - Y_n^{obs}\right)^2}}{\sum_{n=1}^{N} Y_n^{obs}} \tag{10}$$

$$\mathrm{RMSPE} = \sqrt{\frac{1}{N} \cdot \sum_{n=1}^{N} \left(\frac{Y_n^{sim} - Y_n^{obs}}{Y_n^{obs}}\right)^2} \tag{11}$$

$$\mathrm{MPE} = \frac{1}{N} \cdot \sum_{n=1}^{N} \left(\frac{Y_n^{sim} - Y_n^{obs}}{Y_n^{obs}}\right) \tag{12}$$

$$U = \frac{\sqrt{\frac{1}{N} \cdot \sum_{n=1}^{N} \left(Y_n^{sim} - Y_n^{obs}\right)^2}}{\sqrt{\frac{1}{N} \cdot \sum_{n=1}^{N} \left(Y_n^{sim}\right)^2} + \sqrt{\frac{1}{N} \cdot \sum_{n=1}^{N} \left(Y_n^{obs}\right)^2}} \tag{13}$$

$$U_M = \frac{\left(\bar{Y}_n^{sim} - \bar{Y}_n^{obs}\right)^2}{\frac{1}{N} \cdot \sum_{n=1}^{N} \left(Y_n^{sim} - Y_n^{obs}\right)^2} \tag{14}$$

$$U_S = \frac{\left(\sigma^{sim} - \sigma^{obs}\right)^2}{\frac{1}{N} \cdot \sum_{n=1}^{N} \left(Y_n^{sim} - Y_n^{obs}\right)^2} \tag{15}$$

$$U_C = \frac{2 \cdot (1 - p) \cdot \sigma^{sim} \cdot \sigma^{obs}}{\frac{1}{N} \cdot \sum_{n=1}^{N} \left(Y_n^{sim} - Y_n^{obs}\right)^2} \tag{16}$$

4.4. Static calibration

Firstly, a static calibration is illustrated in order to be used as a reference benchmark for comparison with the proposed method. The longest data series (B1695, longer than 3 min) was used for model calibration. It is worth noting that –besides being the longest– this time series includes the most extensive range of speed values. The calibration process was performed within the R software for statistical computing (R Core Team, 2016). In particular, the Improved Stochastic Ranking Evolution Strategy (ISRES) algorithm was used, which is included in the package "nloptr" (Runarsson and Yao, 2005) and is appropriate for nonlinearly constrained global optimization. This method is implemented in a simple way and supports arbitrary nonlinear inequality and equality constraints in addition to the bound constraints. In addition, it incorporates heuristics to escape local optima. On the other hand, although a lots of research has been performed on determining which algorithm is best suited for a given problem, there has not been a satisfactory answer to this question. Thus, various algorithms should be tested in future research.

The objective function that was minimized is: $\mathrm{RMSN}(v_3^{obs}, v_3^{sim})$. The range of model parameters, shown in Table 2, has been defined in an earlier research by Papathanasopoulou and Antoniou (2015). These constraints are defined by Eq. (17):

$$\underline{x}_{it} \leqslant x_{it} \leqslant \bar{x}_{it} \tag{17}$$

which is a special case of Eq. (2). In addition, as initial values for the optimization process, optimal values defined through a sensitivity analysis for Gipps' model and the same data by Papathanasopoulou and Antoniou (2015) were used. However, it is noted that interactions among the parameters had not been taken into account in that sensitivity analysis. However, in this research a global optimization is performed, considering all combinations of these model parameters concurrently. For the whole dataset B1695 the optimization process has converged to the optimal set of parameters after approximately 10000 iterations. The optimal values are presented in Table 2, where "initial values" refers to the model parameter values obtained by Papathanasopoulou and Antoniou (2015) and "optimal values" refers to the parameters obtained from the static

Table 2
Optimization of model parameters using ISRES algorithm.

Parameters of Gipps' model	Parameters range	Initial values	Optimal values
a (m/s^2)	[0.8, 2.6]	0.8	0.8
b (m/s^2)	[−5.2, −1.6]	−5.2	−3.2
V (m/s)	[10.4, 29.6]	14	14.4
s (m)	[5.6, 7.5]	5.6	5.9
$\hat{b}$ (m/s^2)	[−4.5, −3.0]	−3	−3.1
τ (s)	[0.4, 3.0]	0.4	0.4

calibration using the ISRES algorithm within this research. The minimum value of the objective function, namely the RMSN, that was achieved with these optimal values of parameters was 2.2%.

5. Dynamic calibration and results analysis

Gipps' model is calibrated dynamically in order to simulate the speed of the third vehicle ($v_3(t+\tau)$). Gipps' model requires as input data $v_2(t), v_3(t), x_2(t), x_3(t)$ and the appropriate parameter values. The superiority of this calibration over the static calibration presented before is demonstrated both for estimation and also for multiple step prediction of traffic speeds.

5.1. Dynamic calibration

In online calibration an optimization process with the same characteristics (parameters range, initial values, objective function) is iterated per time instant, namely per observation ($v_2(t), v_3(t), x_2(t)$ and $x_3(t)$), and not for the whole data series such as in static calibration. Therefore, a different optimal set of parameters is determined per time instant t in order to be characteristic of the current traffic conditions. In order to simplify the optimization problem, the apparent reaction time is considered equal to $\tau = 0.4$ s (for a discussion and motivation of this choice, see e.g. Papathanasopoulou and Antoniou (2015)). Five parameters are optimized per iteration (the remaining five parameters shown in Table 2).

This implies that –with the addition of subscript t to the time-dependent parameters– in effect Eq. (9) becomes

$$v_{nt}[t+\tau] = min\begin{cases} v_{nt}[t] + 2.5 \cdot a_{nt} \cdot \tau \cdot \left(1 - \frac{v_{nt}[t]}{V_{nt}} \cdot \sqrt{\left(0.025 + \frac{v_{nt}[t]}{V_{nt}}\right)}\right) \\ b_{nt} \cdot \tau + \sqrt{(b_{nt} \cdot \tau)^2 - b_{nt} \cdot \left[2 \cdot (x_{n-1}[t] - s_{n-1,t} - x_n[t]) - v_{nt}[t] \cdot \tau - \frac{v_{n-1}^2[t]}{\hat{b}_t}\right]} \end{cases} \quad (18)$$

where

a_{nt}: the maximum acceleration that the driver of vehicle n wishes to acquire (m/s^2).
b_{nt}: the maximum braking that the driver of vehicle n wishes to apply in order to avoid a crash, $b_n < 0$ (m/s^2).
$\hat{b}_t$: the estimated maximum braking that the driver of the preceding vehicle ($n-1$) wishes to apply (m/s^2).
$s_{n-1,t} = L_{n-1}$ + safety, namely the size of the preceding vehicle ($n-1$) including its length and the safety distance at which vehicle n is unwilling to compromise even when at rest (m).
V_{nt}: the speed at which the driver of vehicle n wishes to travel (m/s).
$x_n[t]$, $x_{n-1}[t]$: the location of the front side of the respective vehicle (n or $n-1$) at time t (m).
$v_{n-1}[t]$: the speed of the preceding vehicle ($n-1$) at time t (m/s).
$v_n[t]$: the speed of the following vehicle (n) at time t (m/s).
τ: the apparent reaction time (a constant for all vehicles) (s).

In setting up the case study, a single objective optimization problem was formulated and the objective function f that was set to be minimized is:

$$\min\ f(\mathbf{x_t}) = \min(\text{RMSN}(v_3^{obs}, v_3^{sim}(\mathbf{x_t}))) \quad (19)$$

where

$$\mathbf{x_t} = (a_{nt}, V_{nt}, b_{nt}, s_{n-1,t}, \hat{b}_t) \quad (20)$$

In the optimization process for the case study, observations of only the previous time instant have been taken into consideration and therefore the formulation of the weights was straightforward, i.e. the weight of the last observation was 1 and that of all previous observations was 0. In Fig. 3, the RMSN goodness-of-fit measure assesses the overall error and performance of the static and dynamic calibration procedures estimating the difference between the observed and the simulated values of speed v_3 per time instant.

RMSN(static) was calculated considering fixed parameters values for all observations. It becomes evident that lower RMSN values are consistently achieved through dynamic calibration, as expected. While the difference is not so large most of the time, there is a specific period, in which the static model seems to perform particularly poorly. In order to investigate the conditions that led to this performance deterioration, we have looked at the prevailing traffic conditions, which indeed provide some insight. In particular, in the bottom subfigure of Fig. 3 observed speeds are also plotted over time, in order to clarify when the static model performance deteriorates. During the time period of interest (the sharp increase in RMSN), very low speeds are observed, and it is therefore reasonable to assume that the static calibration does not allow the model to adapt to these extreme traffic conditions. Therefore, it is not expected to provide a good speed prediction, when significant changes in speed take place. On the other hand, dynamic calibration is more flexible and adaptable to the current traffic conditions, reacting considerably better, even in such extreme situations.

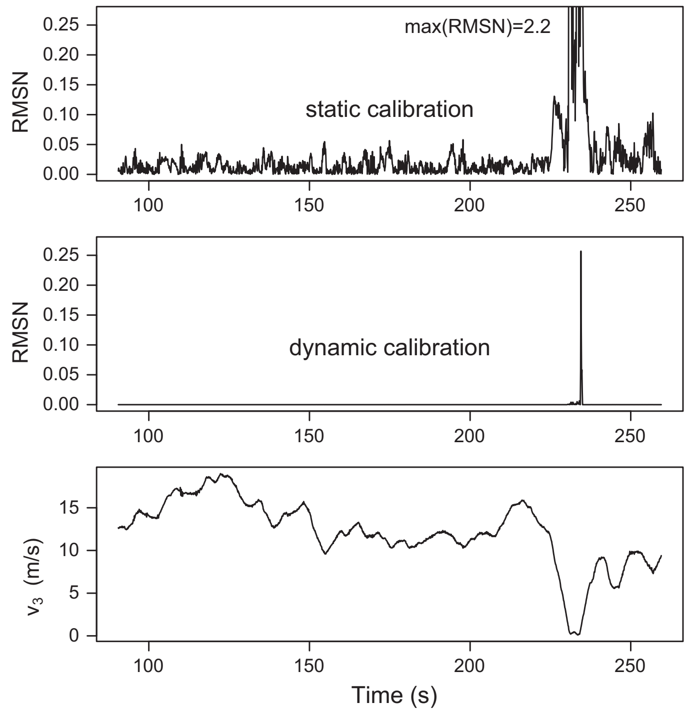

Fig. 3. Dynamic calibration versus static calibration and speed profile (observed values) for B1695 data series.

In this case study, we use a single measure of effectiveness (speed). The failure of the dynamic calibration in the low-speed situation in Fig. 3 could be overcome by considering additional measures of effectiveness (e.g. vehicle gap).

5.2. Multiple time step prediction

Multiple steps prediction is achieved using both methods of calibration, static and dynamic. In each prediction step, predicted values from the previous step and optimal values used in the initial step are imported to the car-following model. However, after the first prediction step, only the speed of the third vehicle v_{3t} is predicted and could be used to the next step. Therefore, the speed v_2 of the lead vehicle, which is also required as input to the model, is considered as constant through the prediction steps, since there is no way to know what the evolution of that speed would be. Extensions to this model could include predicting of other traffic parameters, such as speeds of surrounding vehicles. Values for vehicle positions x_2 and x_3 are calculated according to the distance that was traveled in the corresponding time (i.e. assuming the appropriate speed values).

The proposed methodology has been applied for all data series. In the presentation of the results in the following subsections, we make a distinction between measures of effectiveness and measures of goodness-of-fit that have been used in the objective function, versus those that have not. In particular, the objective function has been formulated in terms of RMSN (as the goodness-of-fit measure) and following car speed (as the measure of effectiveness). Looking only at these metrics could leave us susceptible to over-fitting. However, to demonstrate that this is not the case, we also present results for other measures of effectiveness (in particular distance between the lead and following vehicle), as well as a number of other goodness-of-fitness measures (as described in Section 4.3).

5.2.1. Measures of effectiveness included in the objective function

Fig. 4 presents the aggregate goodness-of-fit measures for the estimated speeds. The left subfigure of Fig. 4 presents the calibration results based on the RMSN metric, which has been included in the objective function. Indeed, as expected, dynamic calibration outperforms static calibration in all cases for one-step prediction. This is evident also from all other goodness-of-fit measures (right subfigure of Fig. 4). The RMSPE measure indicates that using static calibration results in large errors. Values of Theil's inequality U_m and U_s are close to zero for all data series and indicate an ideal fit. It is noted that for the B1695 data series, prediction with the static calibration is using additional information, as the information for the entire data-set has been considered for the estimation of the static parameter values. Therefore, this value is "better" than it would otherwise be. Put differently, the improvement obtained by the dynamic calibration is arguably underestimated. In Fig. 5, the Empirical Cumulative Distribution Functions (ECDFs) of observed and simulated speeds are illustrated. The ECDF of simulated speeds using dynamic calibration is almost identical with the ECDF of observed speeds in the majority of data series.

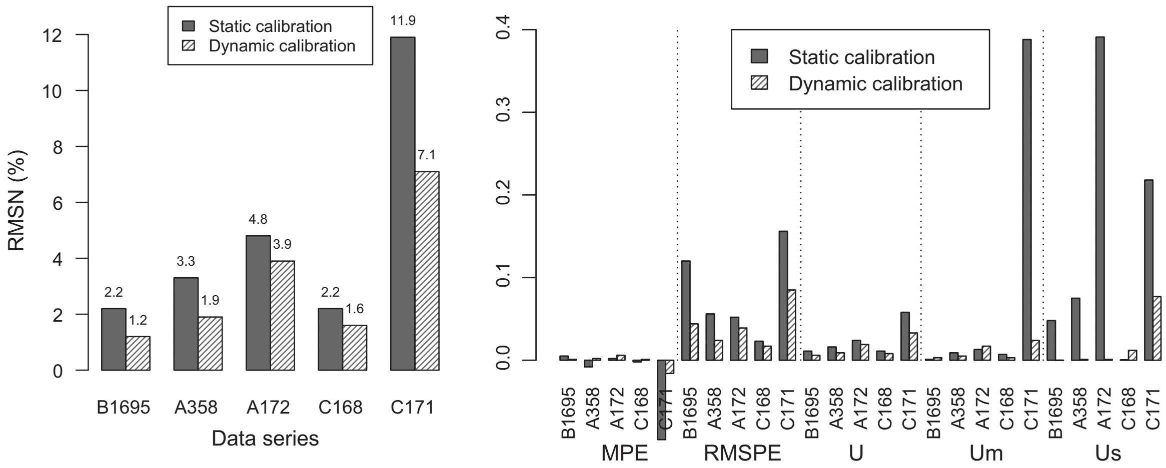

Fig. 4. Comparison of estimated speeds between static and dynamic calibration for one-step prediction.

While in many cases the static calibration also performs reasonably well, in some cases, such as in the first half of data series A172 and C171, the poorer performance of the static calibration (compared to dynamic calibration) is clearly evident.

5.2.2. Measures of effectiveness not included in the objective function

In order to check if the methodology over-fits to speed prediction due to the objective function defined in Eq. (19), other measures of effectiveness such as space, acceleration, etc. not included in the objective function may be checked. For instance, space prediction is not included in the objective function (Eq. (19)) and this could make the parameter estimation rather insensitive to space-gap related properties.

Space headways for dynamic calibration have been estimated using the assumption that the speed v_2 is constant throughout the prediction steps. Fig. 6 is similar to Fig. 4, but this time presents the same results for space headways. Indeed, the dynamic calibration once again performs considerably better than the static calibration, in most cases. Furthermore, Fig. 7 illustrates the Empirical Cumulative Distribution Functions (ECDFs) of the observed and simulated space gaps. Although space gaps were not included as a traffic measure in the objective function, the estimated space gaps from the dynamic calibration track the observed values much better than those obtained from the static calibration.

5.3. Multiple time step prediction results for the entire prediction horizon

The RMSN results for all five data series and for the entire prediction horizon (one- to ten-step prediction) are presented in Fig. 8. The superior performance of the prediction based on the dynamic calibration is evident in all data series. While prediction error consistently increases as the prediction horizon increases, the results obtained from the dynamic calibration never exceed 10% error, even for ten-step prediction into the future.

Fig. 9 presents a more detailed overview of the predicted speeds by the static and dynamic calibration, compared with the observed speed for one of the data series (C171, the one for which the biggest improvement has been achieved through the use of dynamic vs. static calibration).

5.4. Exploration of calibrated parameter values

The overall results presented in the previous subsection eloquently illustrate the superior performance of the dynamic calibration over the static case. In this subsection, we explore the values of the parameters obtained from each approach, in order to gain some further insight. Fig. 10 presents the densities of the obtained parameters for the considered model and data-set. It is noted that, since for each time instant only one of the two equations is critical, the parameter values for that equation are considered at each time point. For example, if the top equation of Eq. (9) is active at the particular point, then the parameters a_{nt} and V_{nt} are used (and therefore these values contribute to the densities in Fig. 10), while if the bottom equation is active then the values for the parameters b_{nt}, s_{nt} and $\hat{b}_t$ are considered.

In each figure, the value of the static calibration is also indicated with a vertical dashed line. It becomes apparent that the dynamic values are not distributed symmetrically around the statically obtained value. This could have several implications. One question could be whether the static calibration is not really optimal. To check for this, we repeated the estimation and prediction using constant parameter values; however, this time, instead of using the value obtained from the static calibration, we used the median from the densities obtained from the dynamic calibration (i.e. the distributions shown in Fig. 10). In that case, the estimation RMSN ended up actually being inferior to that obtained from the static calibration results (with an

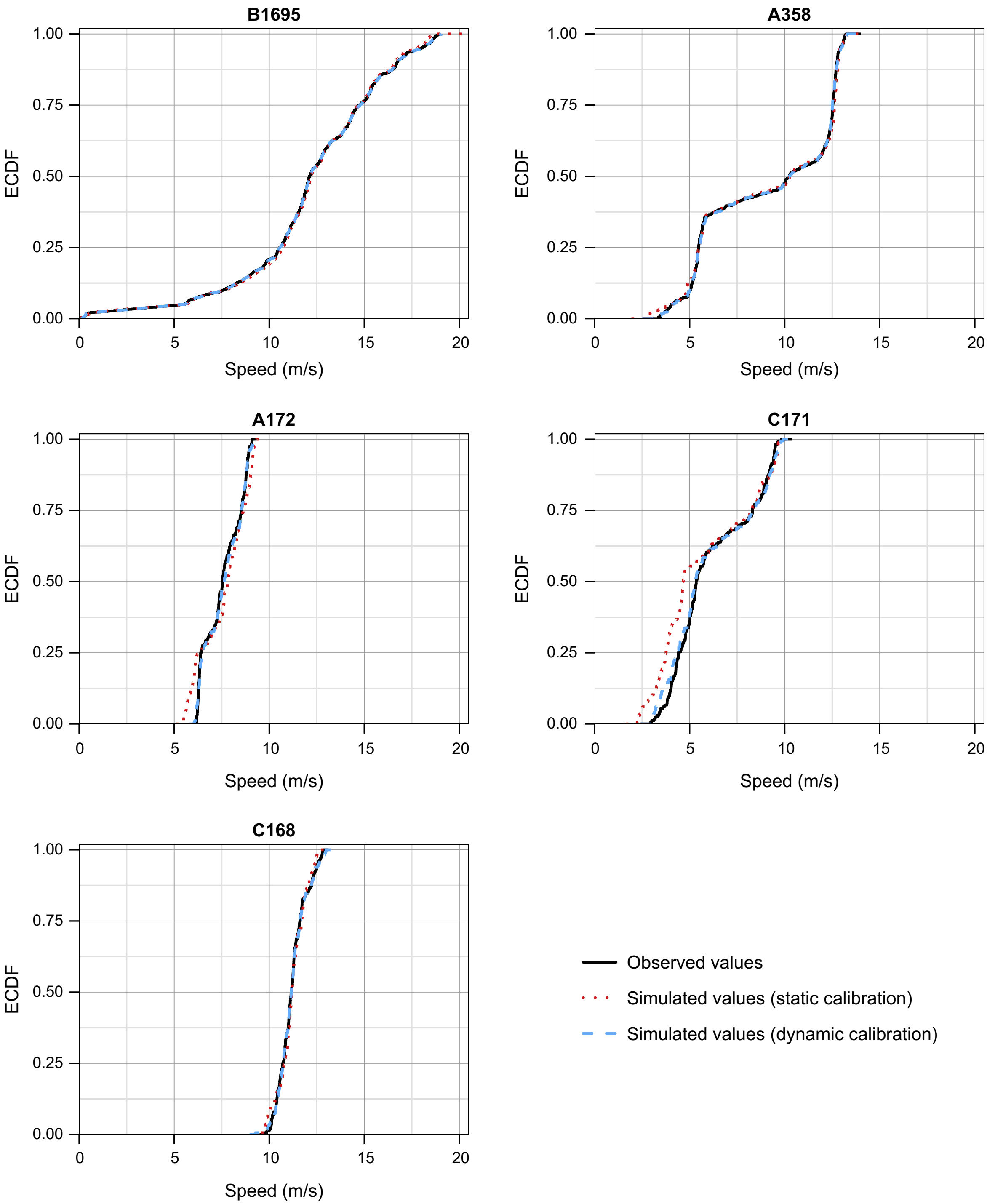

Fig. 5. ECDFs of observed and simulated speeds for one-step prediction.

RMSN of 3.4% instead of 2.2%). Therefore, it seems that there is something different going on, and that indeed the median values from the distributions cannot be used as best values for the determination of constant/average values. The explanation for this may come from the nature of the Gipps model, i.e. the fact that there are two different equations, and at each given time the parameters of a single one are in effect considered. Therefore, while during the dynamic calibration the model steers only these parameters towards their desired values, using the available information, in the case of a static calibration one needs to determine single values that are relevant for all observations.

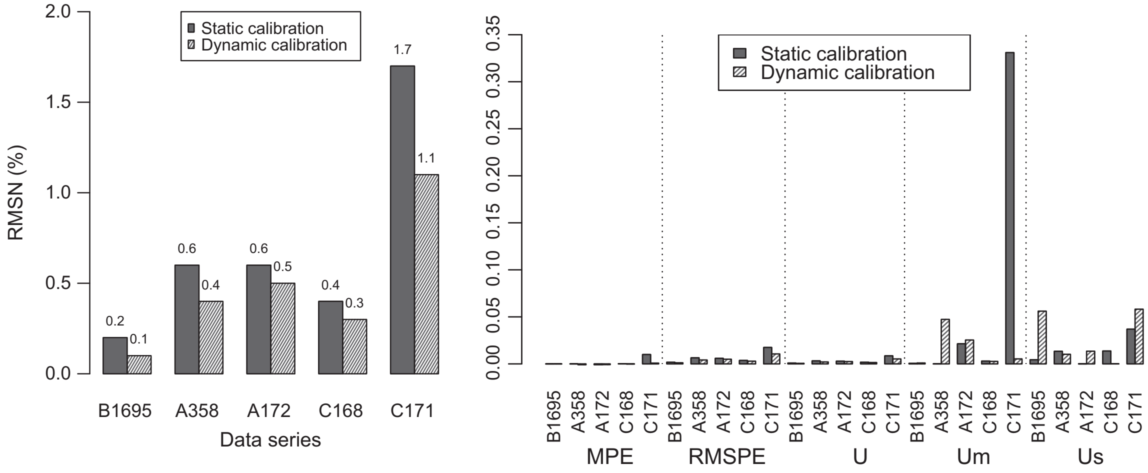

Fig. 6. Comparison of estimated space gaps between static and dynamic calibration for one-step prediction.

Another concern could, of course, be that the dynamic model is actually overfitting. However, the fact that it outperforms the static model even in ten-step predictions (as shown in Fig. 8) provides compelling evidence that this is not the case.

6. Conclusions and future prospects

The findings of this research suggest that dynamic calibration for microscopic traffic models could be promising and should be further studied. In this research, the prediction of the dynamic parameters was simple, in the sense that the dynamically calibrated parameters were assumed as the best available estimate for the short-term values of these parameters. Further research could consider secondary models that would actually aim at predicting the evolution of these parameters, as well, e.g. via autoregressive, polynomial or other statistical forecasting specifications.

Furthermore, the procedure could be applied to other car-following models. Regarding the optimization process, different optimization algorithms could be tested, besides the ISRES optimization algorithm, which has been selected for the case study presented in this research. In addition, the results of this research should be compared with those obtained by a multiobjective optimization process in a future research. While in this research the optimization of the car-following model parameters has been performed using an optimization algorithm across all parameters concurrently, further exploration of the correlation of the model parameters (Kim and Mahmassani, 2011) could provide deeper insight into the problem. The heterogeneity of the drivers and their behavior (Ossen and Hoogendoorn, 2011) could also be further explored, using a larger number of characteristics trajectories from a larger sample of drivers.

While in this case study we only use a small number of vehicles, for which data are available, it is practical to apply this methodology to all individual vehicles in a network, in real time. The computational and data requirements are such, that allow the application of the methodology to each individual vehicle (as the required data could be obtained e.g. from a GPS trace of the vehicle, and e.g. radars/cameras providing information about the vehicles around it). Furthermore, the computational overhead to apply the methodology is minimal and it can be dealt by in-vehicle processing facilities, in a decentralized way. This would allow to not only obtain different parameters estimated and predicted per each vehicle class, but indeed for each individual vehicle, in real time.

In the realistic situation that not all vehicles have the ability to collect/receive the required data, an extrapolation could be used to generalize the obtained results. In this case, it could be practical to identify classes of vehicles, estimate and predict these parameters for the vehicles comprising the sample for each class, and then extrapolate this information to the entire population of vehicles of this class in the studied area. Besides temporal variability of these parameters, by class, one can of course foresee a spatial distribution, as traffic conditions, road characteristics, fleet mix, and other parameters could influence their value.

In the case study, presented in this research, we use a single measure of effectiveness (speed). The failure of the dynamic calibration in the low-speed situation in Fig. 3 could be overcome by considering additional measures of effectiveness (e.g. vehicle gap). Furthermore, the data set used in this research has intentionally considered the movement of vehicles in a single lane, avoiding the complications offered by lane-changing opportunities. Richer data-sets, offering also lane-changing opportunities, would allow the extension of this research to more elaborate models, such as joint car-following/lane-changing models.

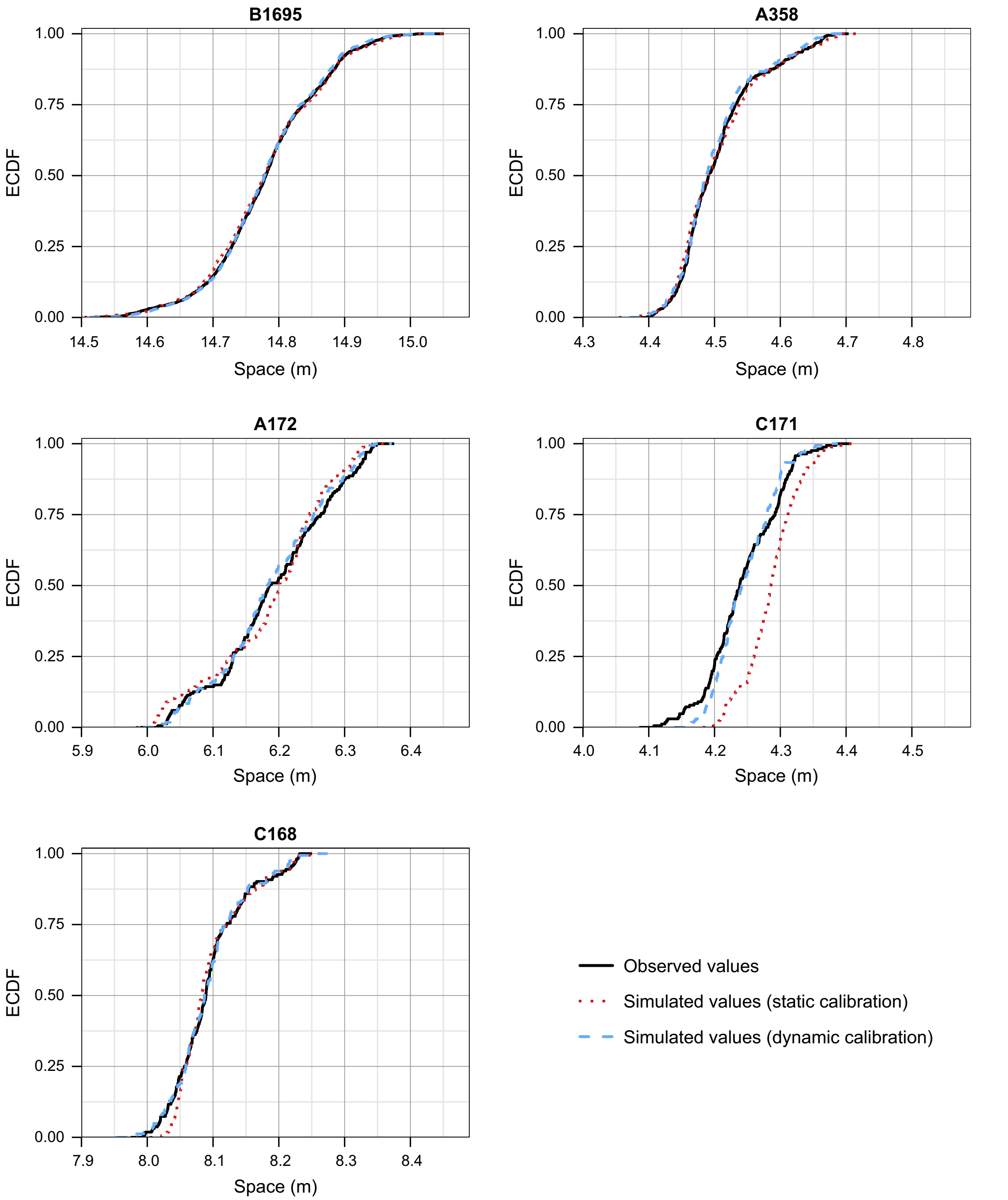

Fig. 7. ECDFs of observed and simulated space gaps for one-step prediction. Note: Different ranges, but same scale, have been used for the *x* axis in all subfigures.

Car-following models are also used as input to Adaptive Cruise Control systems, which also need to be adaptive and consider the heterogeneity of the driver behavior (Bifulco et al., 2013a; Bifulco et al., 2013b). The work presented in this research could be leveraged for the improvement of such models.

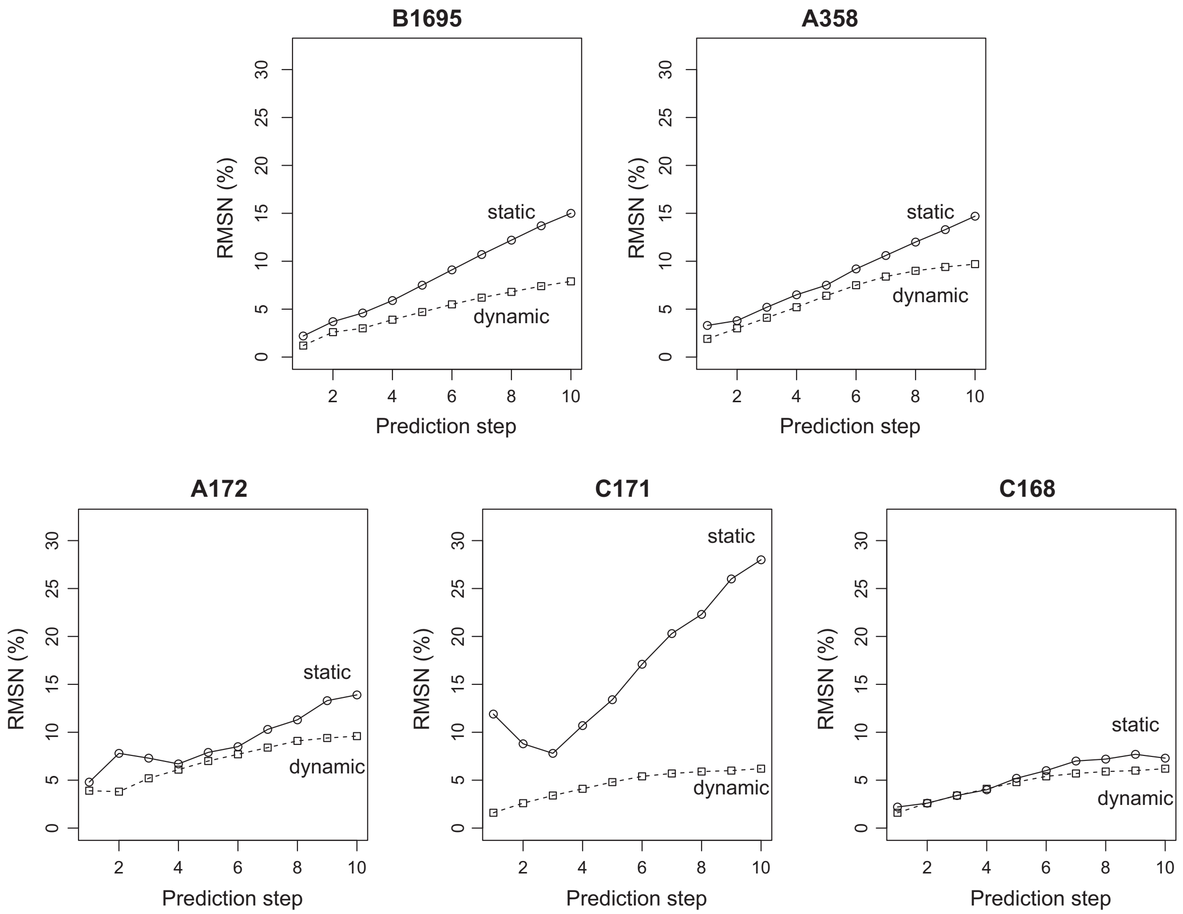

Fig. 8. Multiple time steps prediction using static and dynamic calibration.

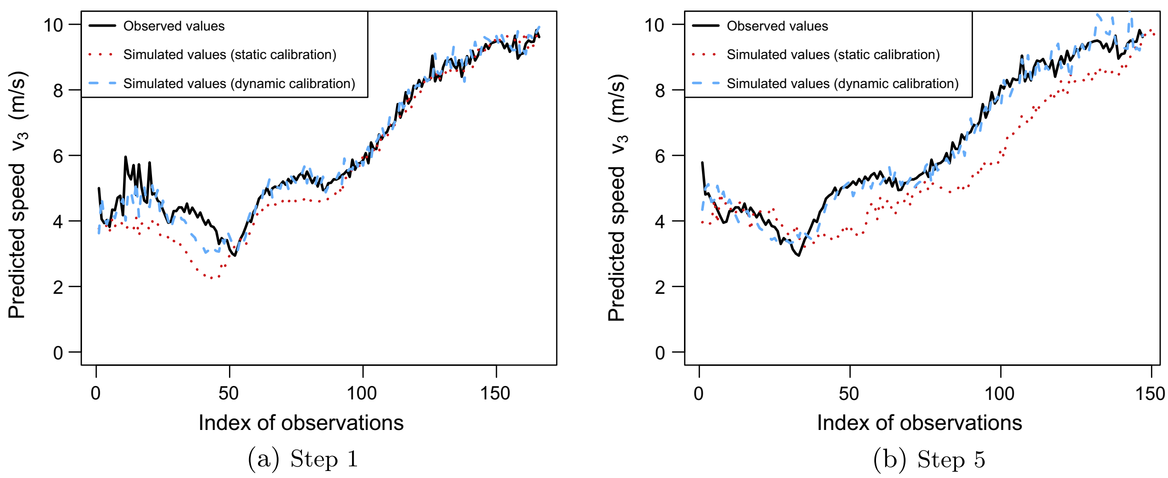

Fig. 9. Predicted speed v_3 for data series C171 for steps 1 and 5.

In conclusion, as we move towards more detailed models, even for online applications, it is expected that dynamic calibration will play an increasing role for this type of models. While a lot of experience exists in the online calibration of macroscopic and mesoscopic models, it is likely that this expertise will not transfer directly to the more detailed microscopic

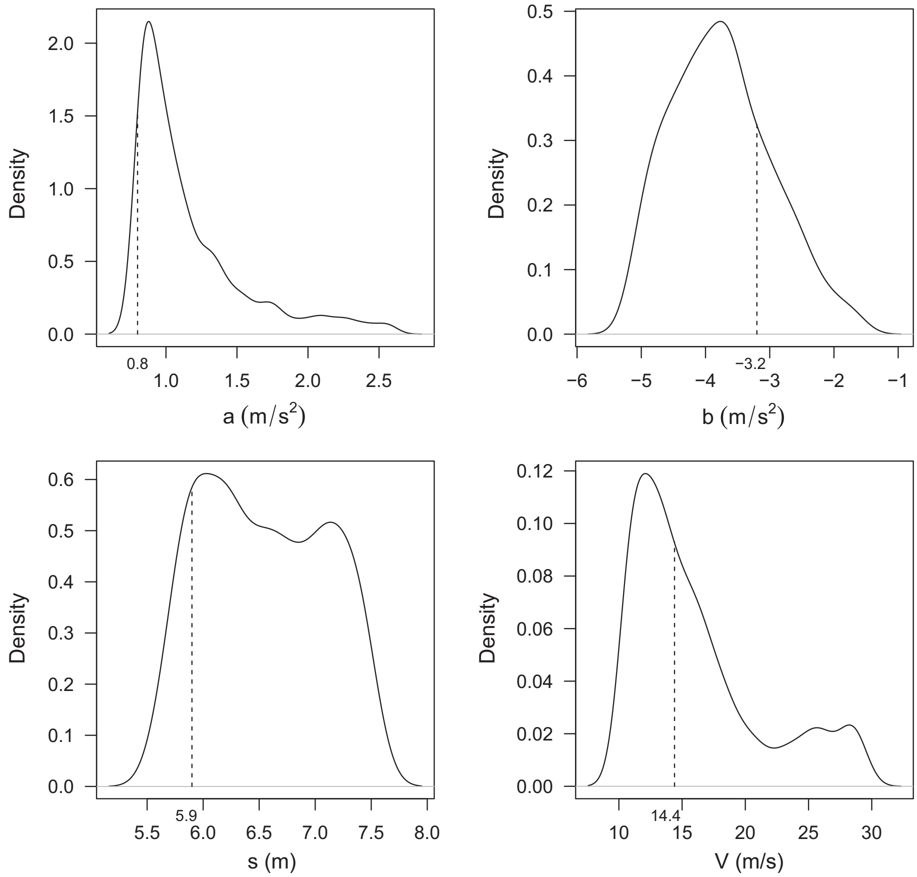

Fig. 10. Distributions of dynamically calibrated parameters. Notes: (i) dashed line: static calibration value and (ii) for each subfigure, only values from instances, in which the corresponding equation is critical, are used.

models. Therefore, novel research is needed, to validate the existing techniques and develop new ones, specifically suited to leverage the benefits and unique characteristics of microscopic traffic simulation models.

Acknowledgments

Research supported by the Action: ARISTEIA-II (Actions Beneficiary: General Secretariat for Research and Technology), co-financed by the European Union (European Social Fund ESF) and Greek national funds. The authors would like to thank Prof. Vincenzo Punzo from the University of Napoli – Federico II for kindly providing the data used in this research.

The first author is thankful for a scholarship by the Alexander S. Onassis Foundation.

References

Antoniou, C., 2004. On-Line Calibration for Dynamic Traffic Assignment. Ph.D. Thesis Department of Civil and Environmental Engineering, Massachusetts Institute of Technology.

Antoniou, C., Balakrishna, R., Koutsopoulos, H.N., 2011. A synthesis of emerging data collection technologies and their impact on traffic management applications. Eur. Trans. Res. Rev. 3, 139–148.

Antoniou, C., Ben-Akiva, M., Koutsopoulos, H.N., 2005. Online calibration of traffic prediction models. Transp. Res. Rec.: J. Transp. Res. Board 1934, 235–245.

Antoniou, C., Ben-Akiva, M., Koutsopoulos, H.N., 2007. Nonlinear Kalman filtering algorithms for on-line calibration of dynamic traffic assignment models. IEEE Trans. Intell. Transp. Syst. 8, 661–670.

Antoniou, C., Koutsopoulos, H., 2006. Estimation of traffic dynamics models with machine-learning methods. Transp. Res. Rec.: J. Transp. Res. Board, 103–111.

Antoniou, C., Koutsopoulos, H.N., Yannis, G., 2013. Dynamic data-driven local traffic state estimation and prediction. Transp. Res. Part C: Emerg. Technol. 34, 89–107.

Aycin, M., Benekohal, R., 1999. Comparison of car-following models for simulation. Transp. Res. Rec.: J. Transp. Res. Board 1678, 116–127.

Balakrishna, R., 2006. Off-Line Calibration of Dynamic Traffic Assignment Models. Ph.D. Thesis Massachusetts Institute of Technology.

Balakrishna, R., Antoniou, C., Ben-Akiva, M., Koutsopoulos, H., Wen, Y., 2007. Calibration of microscopic traffic simulation models: methods and application. Transp. Res. Rec.: J. Transp. Res. Board 1999, 198–207. http://dx.doi.org/10.3141/1999-21.

Barceló, J., Codina, E., Casas, J., Ferrer, J., Garcia, D., 2005. Microscopic traffic simulation: a tool for the design, analysis and evaluation of intelligent transport systems. J. Intell. Rob. Syst. 41, 173–203.

Ben-Akiva, M., Koutsopoulos, H.N., Antoniou, C., Balakrishna, R., 2010. Traffic simulation with DynaMIT. In: Barceló, J. (Ed.), Fundamentals of Traffic Simulation. Springer, pp. 363–398.
Bifulco, G.N., Pariota, L., Brackstione, M., Mcdonald, M., 2013a. Driving behaviour models enabling the simulation of advanced driving assistance systems: revisiting the action point paradigm. Transp. Res. Part C: Emerg. Technol. 36, 352–366.
Bifulco, G.N., Pariota, L., Simonelli, F., Di Pace, R., 2013b. Development and testing of a fully adaptive cruise control system. Transp. Res. Part C: Emerg. Technol. 29, 156–170.
Brackstone, M., McDonald, M., 1999. Car-following: a historical review. Transp. Res. Part F: Traffic Psychol. Behav. 2, 181–196.
Daamen, W., Buisson, C., Hoogendoorn, S.P., 2014. Traffic Simulation and Data: Validation Methods and Applications. CRC Press.
De Fabritiis, C., Ragona, R., Valenti, G., 2008. Traffic estimation and prediction based on real time floating car data. In: 11th International IEEE Conference on Intelligent Transportation Systems (ITSC 2008). IEEE, pp. 197–203.
Ellison, A., Greaves, S., Bliemer, M., 2013. Examining heterogeneity of driver behavior with temporal and spatial factors. Transp. Res. Rec.: J. Transp. Res. Board, 158–167.
Fei, X., Lu, C.-C., Liu, K., 2011. A bayesian dynamic linear model approach for real-time short-term freeway travel time prediction. Transp. Res. Part C: Emerg. Technol. 19, 1306–1318.
Gipps, P.G., 1981. A behavioural car-following model for computer simulation. Transp. Res. Part B: Methodol. 15, 105–111.
Henclewood, D., Suh, W., Rodgers, M., Hunter, M., Fujimoto, R., 2012. A case for real-time calibration of data-driven microscopic traffic simulation tools. In: Simulation Conference (WSC). Proceedings of the 2012 Winter. IEEE, pp. 1–12.
Higgs, B., Abbas, M.M., 2014. Multi-resolution comparison of car-following models using naturalistic data. In: Transportation Research Board 93rd Annual Meeting 14-4528.
Hoogendoorn, S., Ossen, S., Schreuder, M., Gorte, B., 2006. Unscented particle filter for delayed car-following models estimation. In: Intelligent Transportation Systems Conference, 2006. ITSC'06. IEEE. IEEE, pp. 1598–1603.
Hoogendoorn, S.P., Hoogendoorn, R., 2010. Generic calibration framework for joint estimation of car-following models by using microscopic data. Transp. Res. Rec.: J. Transp. Res. Board 2188, 37–45.
Kesting, A., Treiber, M., 2008. Calibrating car-following models by using trajectory data: Methodological study. Transp. Res. Rec.: J. Transp. Res. Board 2088, 148–156.
Kim, J., Mahmassani, H., 2011. Correlated parameters in driving behavior models. car-following example and implications for traffic microsimulation. Transp. Res. Rec.: J. Transp. Res. Board 2249, 62–77.
Kim, Y., 2002. Online Traffic Flow Model Applying Dynamic Flow-Density Relation. Technical Report Int. At. Energy Agency.
Kurzhanskiy, A.A., Varaiya, P., 2010. Active traffic management on road networks: a macroscopic approach. Philos. Trans. R. Soc. London A: Math. Phys. Eng. Sci. 368, 4607–4626.
van Lint, J., Hoogendoorn, S., van Zuylen, H., 2005. Accurate freeway travel time prediction with state-space neural networks under missing data. Transp. Res. Part C: Emerg. Technol. 13, 347–369. http://dx.doi.org/10.1016/j.trc.2005.03.001, <http://www.sciencedirect.com/science/article/pii/S0968090X0500029X>.
Lorkowski, S., Wagner, P., 2005. Parameter calibration of traffic models in microscopic online simulations. In: 84th Annual Meeting of the Transportation Research Board.
Ma, X., 2006. A neural-fuzzy framework for modeling car-following behavior. IEEE International Conference on Systems, Man and Cybernetics, 2006. SMC'06, vol. 2. IEEE, pp. 1178–1183.
Ma, X., Andréasson, I., 2005. Dynamic car following data collection and noise cancellation based on the Kalman smoothing. In: IEEE International Conference on Vehicular Electronics and Safety, 2005. IEEE, pp. 35–41.
Ma, X., Jansson, M., 2007. Model estimation for car-following dynamics based on adaptive filtering approach. In: IEEE Intelligent Transportation Systems Conference (ITSC 2007). IEEE, pp. 824–829.
Miller, M., Skabardonis, A., 2010. San Diego I-15 Integrated Corridor Management (ICM) 7 System: Stage II (Analysis, Modeling, and Simulation). California Path Program, Institute of 8 Transportation Studies. University of California at Berkeley, vol. 9.
Monteil, J., Billot, R., Sau, J., Buisson, C., El Faouzi, N.-E., 2014. Calibration, estimation, and sampling issues of car-following parameters. Transp. Res. Rec.: J. Transp. Res. Board 2422, 131–140.
Olstam, J.J., Tapani, A., 2004. Comparison of Car-Following Models. Swedish National Road and Transport Research Institute, Project VTI meddelande, 960A.
Ossen, S., Hoogendoorn, S., 2005. Car-following behavior analysis from microscopic trajectory data. Transp. Res. Rec.: J. Transp. Res. Board, 13–21.
Ossen, S., Hoogendoorn, S., 2007. Driver heterogeneity in car following and its impact on modeling traffic dynamics. Transp. Res. Rec.: J. Transp. Res. Board, 95–103.
Ossen, S., Hoogendoorn, S.P., 2011. Heterogeneity in car-following behavior: theory and empirics. Transp. Res. Part C: Emerg. Technol. 19, 182–195.
Papageorgiou, M., Blosseville, J.-M., Hadj-Salem, H., 1989. Macroscopic modelling of traffic flow on the Boulevard Périphérique in Paris. Transp. Res. Part B: Methodol. 23, 29–47.
Papathanasopoulou, V., Antoniou, C., 2015. Towards data-driven car-following models. Transp. Res. Part C: Emerg. Technol. 55, 496–509.
Pereira, F.C., Antoniou, C., Fargas, J.A., Ben-Akiva, M., 2014. A metamodel for estimating error bounds in real-time traffic prediction systems. IEEE Trans. Intell. Transp. Syst. 15, 1310–1322.
Punzo, V., Ciuffo, B., Montanino, M., 2012. Can results of car-following model calibration based on trajectory data be trusted? Transp. Res. Rec.: J. Transp. Res. Board 2315, 11–24.
Punzo, V., Formisano, D.J., Torrieri, V., 2005. Part 1: Traffic flow theory and car following: Nonstationary Kalman filter for estimation of accurate and consistent car-following data. Transp. Res. Rec.: J. Transp. Res. Board 1934, 1–12.
R Core Team, 2016. R: A Language and Environment for Statistical Computing. R Foundation for Statistical Computing Vienna, Austria. (URL: <http://www.R-project.org/>).
Rahman, M., Chowdhury, M., Khan, T., Bhavsar, P., 2014. A parameter estimation and calibration method for car-following models. In: Transportation Research Board 93rd Annual Meeting 14-4634.
Runarsson, T.P., Yao, X., 2005. Search biases in constrained evolutionary optimization. IEEE Trans. Syst. Man Cybern. Part C: Appl. Rev. 35, 233–243.
Schultz, G., Rilett, L., 2004. Analysis of distribution and calibration of car-following sensitivity parameters in microscopic traffic simulation models. Transp. Res. Rec.: J. Transp. Res. Board 1876, 41–51.
Treiber, M., Kesting, A., 2013. Microscopic calibration and validation of car-following models-a systematic approach. Procedia-Soc. Behav. Sci. 80, 922–939.
Vlahogianni, E.I., Karlaftis, M.G., Golias, J.C., 2005. Optimized and meta-optimized neural networks for short-term traffic flow prediction: a genetic approach. Transp. Res. Part C: Emerg. Technol. 13, 211–234. http://dx.doi.org/10.1016/j.trc.2005.04.007, <http://www.sciencedirect.com/science/article/pii/S0968090X05000276>.
Vlahogianni, E.I., Karlaftis, M.G., Golias, J.C., 2008. Temporal evolution of short-term urban traffic flow: a nonlinear dynamics approach. Comput.-Aided Civ. Inf. Eng. 23, 536–548.
Wagner, P., 2012. Analyzing fluctuations in car-following. Transp. Res. Part B: Methodol. 46, 1384–1392.